# Rock magnetism of quartz and feldspars chemically separated from pelagic red clay: a new approach to provenance study



Usui *et al. Earth, Planets and Space (2018) 70:153*
https://doi.org/10.1186/s40623-018-0918-1

Earth, Planets and Space

FULL PAPER Open Access

# Rock magnetism of quartz and feldspars chemically separated from pelagic red clay: a new approach to provenance study

Yoichi Usui[1*], Takaya Shimono[2] and Toshitsugu Yamazaki[3]

**Abstract**

Magnetic mineral inclusions in silicates are widespread in sediments as well as in igneous rocks. Because they are isolated from surrounding environment, they have potential to preserve original magnetic signature even in chemically altered sediments. Such inclusions may provide proxies to help differentiating the source of the host silicate. We measure magnetism of quartz and feldspars separated by chemical digestion of pelagic red clay. The samples are from the upper 15 m of sediments recovered at Integrated Ocean Drilling Program Site U1366 in the South Pacific Gyre. The quartz and feldspars account for 2.3–22.7 wt% of the samples. X-ray diffraction analyses detect both plagioclase feldspar and potassium feldspar. Plagioclase is albite-rich and abundant in the top ~ 7.4 m of the core. Potassium feldspar mainly occurs below ~ 10.4 m. The dominance of albite-rich plagioclase differs from a previous investigation of coarser fraction of sediments from the South Pacific. Saturation isothermal remanence (SIRM) intensities of the quartz and feldspars are $7.45 \times 10^{-4}$ to $1.98 \times 10^{-3}$ $Am^2/kg$, accounting for less than 1.02% of the SIRM of the untreated bulk samples. The depth variations of the silicate mineralogy and the previously reported geochemical end-member contributions indicate that quartz and/or plagioclase above 8.26 m is likely to be Australian dust. In contrast, the relative abundance and the magnetic properties of quartz and feldspars vary below 10.42 m, without clear correlation with geochemical end-member contributions. We consider that these changes trace a subdivision of the volcanic component. Our results demonstrate that magnetism of inclusions can reveal additional information of mineral provenance, and chemical separation is an essential approach to reveal the environmental magnetic information carried by magnetic inclusions.

**Keywords:** Magnetic inclusions, South Pacific Gyre, Eolian dust, Environmental magnetism

## Introduction

Provenance of the eolian component in pelagic sediments can constrain long-term change in the wind direction over the oceans and climate condition on land (e.g., Leinen and Heath 1981; Kyte et al. 1993; Rea 1994; Grousset and Biscaye 2005). Most frequently, geochemical methods such as isotopic composition have been employed to characterize the eolian component (e.g., Nakai et al. 1993; Asahara et al. 1999; Pettke et al. 2000; Stancin et al. 2008; Hyeong et al. 2016). Analysis of major, trace, and rare earth element concentrations in bulk sediments combined with multivariate statistical modeling is also an effective approach to distinguishing multiple eolian sources to the sediments (e.g., Leinen and Heath 1981; Kyte et al. 1993; Dunlea et al. 2015a). The composition of sediments is compared with modern surface sediments and/or known dust sources to "fingerprint" the sediments and to estimate the source. For example, relatively higher 87Sr/86Sr and 143Nd/144Nd ratios are often correlated with old, felsic continental source such as Asian and Australian dust relative to young, mafic volcanic source such as arc volcanoes. Although such geochemical fingerprinting is a powerful tool, the correlation with specific source is empirical, especially for ancient sediments. Therefore, it is recommended to combine

*Correspondence: yoichi@jamstec.go.jp
[1] Department of Deep Earth Structure and Dynamics Research, Japan Agency for Marine-Earth Science and Technology, Natsushima-cho, Yokosuka, Kanagawa, Japan
Full list of author information is available at the end of the article

multiple proxies to enhance the reliability and accurately characterize the eolian component (Grousset and Biscaye 2005).

Magnetic properties have also been used to constrain the provenance of magnetic minerals in fluvial sediments (Oldfield et al. 1985), loess (Maher et al. 2009; Liu et al. 2015), marine sediments (Bloemendal et al. 1992), and ice cores (Lanci et al. 2008). Magnetism records rich information about abundance, composition, grain size, and grain shape of magnetic minerals, that can differentiate the provenance (e.g., Thompson and Oldfield 1986; Liu et al. 2012). Complexity arises, however, as the magnetic mineralogy of sediments can be modified during transport and after deposition (e.g., Maher 2011). On land, new magnetic minerals may be formed as ultrafine hematite coating in arid area (Potter and Rossman 1979) or pedogenic magnetic minerals (Zhou et al. 1990). Within sedimentary column, Fe-oxides often undergo reductive dissolution or oxidation depending on the redox condition of the sediments (e.g., Roberts 2015). There is evidence that new magnetic authigenic and biogenic minerals may form via microbial activity (Petersen et al. 1986; Stolz et al. 1986; Lovley et al. 1987). Although these changes in magnetic mineralogy carry paleoenvironmental information, they often destroy or mask the primary source characteristics of the eolian component. Consequently, successful applications of magnetism to the provenance study mostly come from recent or quaternary materials, where minimal modification of magnetic minerals is expected.

Several studies demonstrated that sediments contain silicate-hosted magnetic mineral inclusions (Hounslow and Maher 1996; Caitcheon 1998; Maher et al. 2009; Chang et al. 2016c; Zhang et al. 2018). For some igneous rocks, the magnetic inclusions in silicate, especially plagioclase, are found to be similar in mineralogy with the corresponding whole rocks (e.g., Cottrell and Tarduno 1999, 2000). The magnetic inclusions are separated from external environment by the host silicate; thus, they can preserve the original signature as long as the host silicates survive (e.g., Hounslow and Morton 2004; Tarduno et al. 2006). The mineralogy of the host silicates in sediments has been identified using magnetic extraction techniques. The reported host minerals include feldspars, quartz, pyroxenes, and possibly amphiboles and chlorite (Hounslow and Maher 1996; Chang et al. 2016c). Hounslow and Maher (1996) also reported common occurrence of apatite, barite, and pyrite in their magnetic extract. Magnetic extraction gathers both discrete magnetic minerals and silicate-hosted inclusions, so magnetism of the silicate-hosted inclusions cannot be studied by this technique alone. Previous studies of fluvial sediments successfully fingerprinted different sources by chemically digesting the discrete magnetic minerals to isolate the silicates with magnetic inclusions (Alekseeva and Hounslow 2014; Hounslow and Morton 2004; Maher et al. 2009). For marine sediments, the magnetism of magnetic inclusions has been only assessed via analysis of bulk magnetic measurements of pelagic carbonate (Chen et al. 2017) and pelagic red clay (Zhang et al. 2018). Consequently, the detailed magnetic characteristics and the host mineral phases have not been well resolved. While it is proposed that magnetic inclusions can contribute to the magnetism of bulk sediments (Chang et al. 2016c) especially for reducing environment (Chang et al. 2016a), direct quantification of the magnetic intensity of inclusions is lacking. In this study, we apply chemical digestion techniques to pelagic marine sediments to directly characterize the silicate-hosted magnetic inclusions, and to test the applicability of magnetic inclusions in provenance studies of such sediments.

## Samples and geological background

We examine sediments from Integrated Ocean Drilling Program (IODP) Site U1366. The site was drilled during Expedition 329 in the South Pacific Gyre (Fig. 1a). The sediments are mostly composed of red-brownish pelagic clay (Expedition 329 Scientists 2011). The pore water is oxic throughout the sediment column (D'Hondt et al. 2015). Detailed stratigraphic correlation among multiple Holes at Site U1336 is not available, but the lithostratigraphy is expected to be consistent among Holes (Expedition 329 Scientists 2011). The sediments are divided into two lithostratigraphic Units I and II. Unit I is subdivided into three Subunits Ia, Ib, and Ic. The major lithology of Subunit Ia and Ic is zeolitic metalliferous clay, while Subunit Ib contains little amount of zeolite and high amount of oxide. Unit II is only recognized in Hole 1366F, and characterized by very dark color and the absence of zeolite. Dunlea et al. (2015a) statistically analyzed the chemical composition of sediments from Site U1366 and the other sites drilled during the Expedition 329, and modeled the compositional variations using end-member components. They identified two eolian end-members: a component similar to post-Archean average Australian shale (PAAS), and a component similar to rhyolite. The former was interpreted as dust from Australia, and the latter as volcanic ash. The contribution of the "PAAS" end-member increases up-core roughly from Subunit Ib (Fig. 1b). Using a cobalt-based age model (Dunlea et al. 2015b) which assumes constant non-detrital cobalt flux, this trend was interpreted to reflect drying of Australia since Early Eocene. The contribution of the "rhyolite" end-member does not show clear secular trend. We focus on samples from the top 15 m of Hole U1366C that covers Subunit Ia, Ib, and Ic. At Site U1365 which is

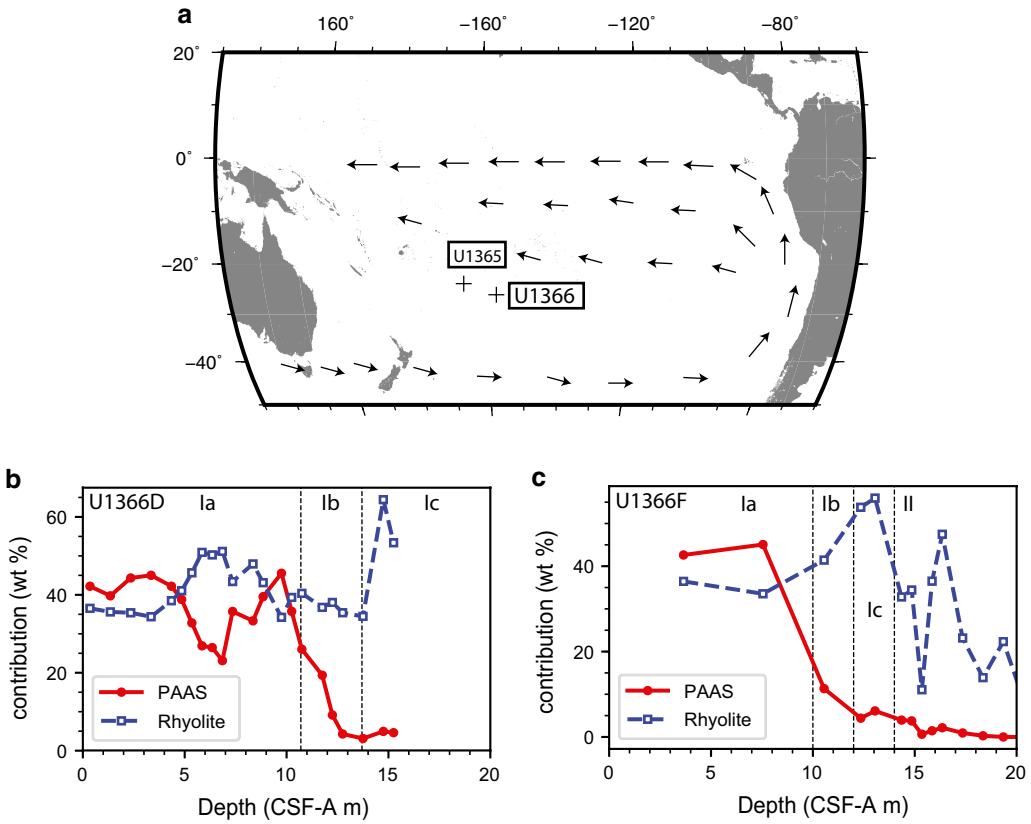


**Fig. 1** Site locations and geochemical estimates of the eolian components. **a** A map showing the locations of Sites U1366 and U1365. Arrows indicate schematic annual average wind directions. **b**, **c** Depth variation of the contributions of the eolian geochemical end-members at Hole U1366D (**b**) and Hole U1366F (**c**) (Dunlea et al. 2015a). Red solid circles represent the "PAAS" end-member and blue open squares "rhyolite" end-member. Vertical dashed lines show the location of lithostratigraphic unit boundaries

~900 km west from Site U1366, Shimono and Yamazaki (2016) reported that magnetism of bulk sediments is largely controlled by magnetofossils, especially in sediments older than ~23 Ma.

Several studies investigated the origin of quartz and feldspars in surface pelagic sediments in the South Pacific (Rex and Goldberg 1958; Peterson and Goldberg 1962; Clayton et al. 1972; Mokma et al. 1972). The abundance, grain size, and oxygen isotope ratios of quartz indicate that most of this mineral in the western and central South Pacific is from Australia and New Zealand by eolian transport (Rex and Goldberg 1958; Clayton et al. 1972; Mokma et al. 1972), although some large (>32 μm) quartz crystals may be from local volcanoes (Peterson and Goldberg 1962). Peterson and Goldberg (1962) discussed that feldspars in the South Pacific are mostly volcanic origin based on the geographical distribution of different types of feldspars and their close relationship with palagonite. However, they investigated feldspar crystals in size fractions of >32 and 4–8 μm, while the mode of the grain size distribution of South Pacific pelagic clay is ~2 μm for quartz (Mokma et al. 1972) and clay minerals (Rea and Bloomstine 1986). Therefore, the origin of the bulk of feldspars in the area has not yet resolved.

## Methods

### Chemical separation

Overall, we employ sodium pyrosulfate ($Na_2S_2O_7$) fusion technique to separate quartz and feldspars from the bulk sediments (Syers et al. 1968; Clayton et al. 1972; Blatt et al. 1982; Stevens 1991). Dry samples of ~0.3 g were first treated with citrate-sodium dithionite solution buffered with sodium bicarbonate to remove poorly crystalline Fe–Mn oxides as well as fine-grained discrete magnetite (Rea and Janecek 1981; Hunt et al. 1995). The residues were freeze-dried and heated with $Na_2S_2O_7$ to 460 °C, and then treated with 3 N HCl and washed with purified water. Then, the residues were heated to 80 °C in 1 M NaOH overnight and washed with purified water. X-ray diffraction (XRD) analysis was conducted using a diffractometer Rigaku MiniFlex II with Cu Kα radiation at JAMSTEC to check the effectiveness of the chemical

separation, and to evaluate feldspar mineralogy and qualitative abundance of mineral phases. Relative abundances of minerals were estimated by the reference intensity ratio method (Hubbard et al. 1976) using software Rigaku PDXL. Note that, during these process, subtle modifications of inclusions may have been occurred such as magnetic domain state relaxation or alteration of thermally unstable minerals, although the effect on overall magnetism is often small compared to the stable magnetic inclusions (e.g., Tarduno et al. 2006). Therefore, the quartz and feldspars separates should be viewed as operationally defined materials.

### Magnetic measurements

We analyzed the processed samples as well as untreated bulk sediment samples for comparison. To estimate the abundance of magnetic minerals, we measured mass-specific anhysteretic remanence (ARM) and saturation isothermal remanence (SIRM). ARM was imparted using cryogenic magnetometer systems at JAMSTEC (2G Enterprises 755R) and the Geological Survey Japan (GSJ) (2G Enterprises 760) with a peak alternating field of 80 mT and a DC bias field of 0.1 mT. IRM was imparted using a pulse magnetizer (2G Enterprises 660) with a 2.5 or 2.7 T field at JAMSTEC and GSJ. Remanences were measured using the cryogenic magnetometers. Some of the SIRM of the untreated samples were measured using a spinner magnetometer (Natsuhara-Giken SMM-85) at GSJ.

To characterize magnetic minerals, we examined the ratio of ARM susceptibility to SIRM (kARM/SIRM) and S ratios. The value of kARM/IRM depends on magnetic grain size (Robinson 1986) and magnetostatic interaction (Cisowski 1981), with smaller values indicate larger grain size and/or larger magnetostatic interaction. We used two back field magnitudes of 0.1 and 0.3 T to calculate two $S$ ratios, $S_{-0.1}$ and $S_{-0.3}$, respectively. $S_{-0.3}$ measures the fraction of magnetization not carried by high-coercivity antiferromagnetic minerals such as hematite and goethite. $S_{-0.1}$ measures the fraction of low coercivity mineral magnetization. For fine-grained titanomagnetite expected to present in pelagic sediments, higher $S_{-0.1}$ (lower coercivity of remanence) can be related to higher titanium content (Day et al. 1977) as well as lower abundance of single-domain grains. To further estimate magnetic mineralogy, we examined low-temperature magnetism using a Quantum Design MPMS-XL5 magnetometer at the Center for Advanced Marine Core Research, Kochi University. Samples were first cooled from 300 to 6 K in 5 T field; then, the temperature dependence of the remanence, $m(T)$, was measured upon heating to 300 K in zero field.

## Results

### Chemical separation

The chemical separate is white powders, and optical microscopic observations show that it consists of transparent particles with typical size of a few μm (Fig. 2a). The chemically extracted quartz and feldspars make up 2.3–22.7 wt% of the bulk sediments (Table 1). These values are broadly consistent with the quartz content in surface sediments at site MSN 125G (26°01′S, 155°59′W; ~1000 km east from Site U1366) and site MSN116P (35°50′S, 163°01′W; ~1350 km south–southeast from Site U1366) that are 5 and 19%, respectively (Clayton et al. 1972; Mokma et al. 1972). The content is markedly low in lithostratigraphic Subunit Ib with an average of 6.8 wt% (Fig. 2b).

XRD analyses indicate that the mineral separates consist of quartz and feldspars (Fig. 3). Peaks corresponding to both plagioclase feldspar and potassium feldspar were detected (Fig. 3d). Peterson and Goldberg (1962)

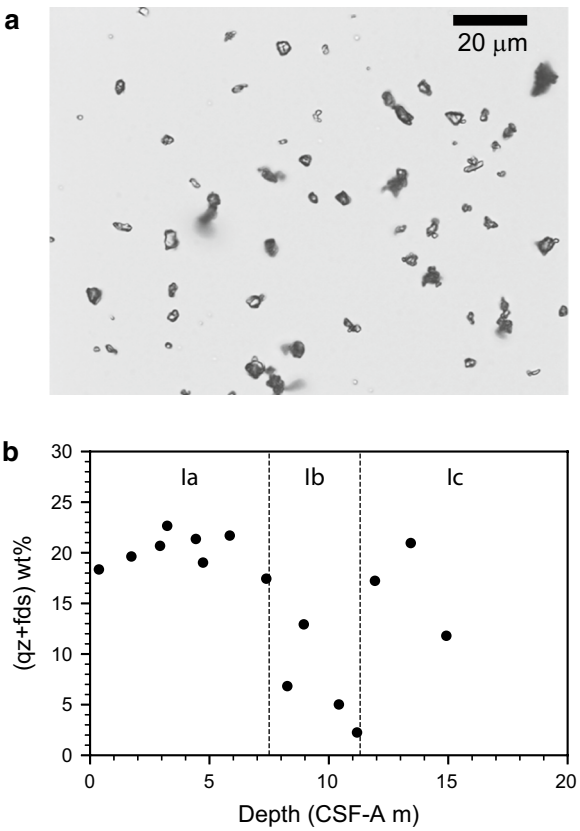


**Fig. 2** **a** Representative optical microscope image of the quartz feldspars separate from sample from 0.37 CSF-A m. **b** Depth variation of the mass fraction of the quartz and feldspars separate. Vertical dashed lines represent lithostratigraphic unit boundaries

**Table 1 Summary of the characteristics of quartz and feldspars**

| Depth (CSF-A m) | Mass fraction (wt%) | ARM ($10^{-5}$Am$^2$/kg) | SIRM ($10^{-3}$Am$^2$/kg) | kARM/SIRM (mm/A) | $S_{-0.1}$ | $S_{-0.3}$ | Lithostratigraphic unit |
|---|---|---|---|---|---|---|---|
| 0.37 | 18.4 | 3.05 | 0.745 | 0.33 | 0.70 | 0.94 | Ia |
| 1.73 | 19.6 | 3.51 | 0.750 | 0.37 | 0.74 | 0.97 | Ia |
| 2.93 | 20.7 | 3.83 | 0.894 | 0.34 | 0.71 | 0.95 | Ia |
| 3.23 | 22.7 | 3.41 | 0.745 | 0.36 | 0.76 | 0.97 | Ia |
| 4.43 | 21.4 | 3.36 | 0.614 | 0.44 | 0.68 | 0.93 | Ia |
| 4.73 | 19.0 | 2.66 | 0.489 | 0.43 | 0.69 | 0.95 | Ia |
| 5.85 | 21.7 | 3.80 | 1.049 | 0.29 | 0.80 | 0.96 | Ia |
| 7.38 | 17.4 | 4.88 | 0.624 | 0.62 | 0.80 | 0.96 | Ia |
| 8.26 | 6.8 | 4.34 | 0.795 | 0.43 | 0.74 | 0.92 | Ib |
| 10.42 | 5.0 | 13.52 | 1.720 | 0.63 | 0.86 | 0.97 | Ib |
| 11.18 | 2.3 | 7.58 | 1.306 | 0.46 | 0.82 | 0.96 | Ib |
| 11.93 | 17.2 | 17.58 | 1.353 | 1.03 | 0.93 | 0.99 | Ic |
| 13.43 | 21.0 | 27.01 | 1.983 | 1.08 | 0.93 | 0.99 | Ic |
| 14.92 | 11.8 | 20.41 | 1.616 | 1.01 | 0.89 | 0.95 | Ic |

determined the plagioclase composition in surface sediments from the South Pacific using the separation between (131) and ($1\bar{3}1$) peaks (Goodyear and Duffin 1954). In our samples, the ($1\bar{3}1$) peak was obscured by overlapping nearby peaks. Nonetheless, the separation is clearly less than 1.5°, pointing to albite-rich composition. This is further checked using the separations between (111) and ($1\bar{1}1$), and ($\bar{1}32$) and (131) (Smith 1956). The separations were ~0.5°–0.6° and ~2.5°–2.6°, respectively (Fig. 3e). These values also correspond to albite-rich composition with anorthosite content of 0–20% (Smith 1956).

The peak positions do not vary much with depth, but relative intensities do. We estimate the mineral abundance using peaks around 13.8°, 14.9°, 20.8°, 22.0°, and 30.4° assuming mixing of quartz (Dušek et al. 2001), low albite (Armbruster et al. 1990), and sanidine (Marcille et al. 1993) (Fig. 4). Potassium feldspar is detected below 7.38 m, and its abundance broadly decreases up-core. The abundance of plagioclase sharply increases between 8.26 and 7.38 m. The abundance of quartz is low below 13.43 m. These patterns correspond to lithostratigraphic changes; Subunit Ia is characterized by the abundant plagioclase. Subunits Ib and Ic are transitional toward more potassium feldspar-rich composition down core, but Subunit Ib appears to contain fewer plagioclase relative to quartz.

### Magnetic measurements

The magnetic data of the quartz and feldspars are summarized in Table 1, and that of the untreated bulk samples are in Table 2. The ARM intensities of the quartz and feldspars range from $3.05 \times 10^{-5}$ to $2.70 \times 10^{-4}$ Am$^2$/kg, and SIRM intensities from $7.45 \times 10^{-4}$ to $1.98 \times 10^{-3}$ Am$^2$/kg (Table 1). Together with the mass fraction of the quartz and feldspars, these values correspond to less than 1.02% of remanence intensity of untreated bulk samples. Both ARM and SIRM are higher and generally decreasing up-core to 10.42 m, and stay nearly constant above 8.26 m (Fig. 5). The kARM/SIRM values of the quartz and feldspars range from 0.326 to 1.08 mm/A, which is significantly lower than the values of untreated samples (0.839–2.29 mm/A; Fig. 6a, b), possibly reflecting the digestion of biogenic magnetite. The kARM/SIRM values of the quartz and feldspars drop from Subunit Ic to Ib, while for untreated samples it is from Subunit Ib to Ia. The S ratios of the quartz and feldspars are lower than that of untreated samples (Fig. 6c, d), which is also explained by the loss of relatively low coercivity biogenic magnetite. Still, the $S_{-0.3}$ values are high, indicating that antiferromagnetic minerals such as hematite do not contribute much to the magnetism of the quartz and feldspars. The $S_{-0.1}$ values are higher in Subunit Ic (~0.9) and decrease toward Subunit Ia (~0.75); within Subunit Ia, the $S_{-0.1}$ values do not vary much.

Low-temperature measurements of the quartz and feldspars detect the Verwey transition of magnetite at around 120 K, while untreated samples do not show the transition (Fig. 7a–c). The Verwey transition temperature of 120 K is consistent with some bulk sediments from elsewhere containing detrital magnetite (Chang et al. 2016b). The absence of the clear Verwey transition in untreated samples is consistent with the behavior reported from Site U1365 (Shimono and Yamazaki 2016), and most likely it reflects oxidation of discrete magnetic minerals in the oxic sediments. The magnitude of the demagnetization associated with the Verwey transition in the quartz and feldspars appears to vary with depth (Fig. 7d). We quantify the demagnetization magnitude as follows

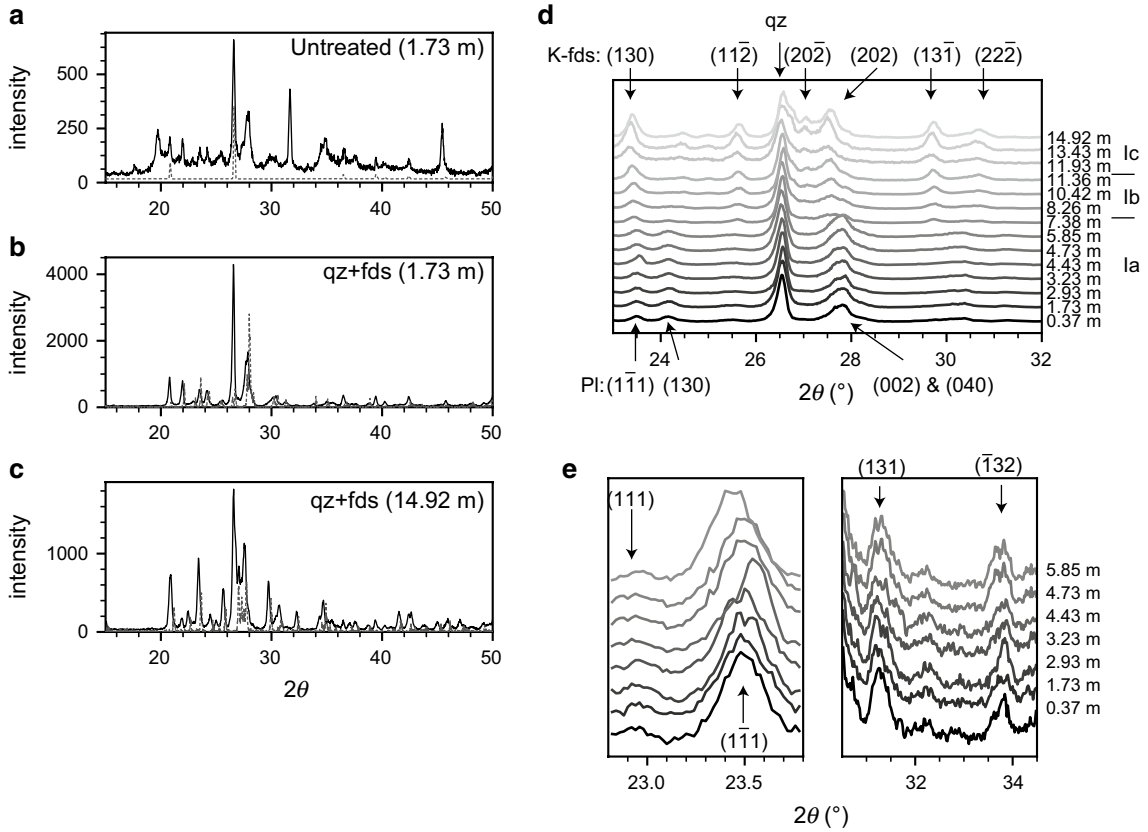


**Fig. 3** Results of XRD analyses. **a**–**c** Representative diffractograms of untreated sample from 1.73 m (**a**), quartz and feldspars from 1.73 m (**b**), and quartz and feldspars from 14.92 m (**c**). Dashed lines represent reference diffraction patterns for quartz (**a**; RRUFFID = R110108), albite (**b**; RRUFFID = R040068), and sanidine (**c**; RUFFID = R060313) in arbitrary scale. Data are downloaded from RRUFF project (http://rruff.info/). **d** Depth variation of the diffractograms for quartz and feldspars showing changing contribution of potassium feldspar and plagioclase. Each diffractograms are normalized by the peak of quartz (qz). Some peak identifications were given for potassium feldspar (K-fds) and plagioclase (pl) on the top and bottom of the plot, respectively. **e** Blowup of diffractograms for plagioclase composition determination using the separations between (111) and (1$\bar{1}$1) (left), and (1$\bar{3}$2) and (131) (right)

(Fig. 7e). First, we fit a straight line to the remanence between 130 and 150 K. Then, we extrapolated the line to 80 K to calculate an expected remanence, $m_{\mathrm{est}}$ (80 K). Finally, the demagnetization magnitude is approximated by the difference $m(80\ \mathrm{K}) - m_{\mathrm{est}}$ (80 K) normalized by $m$(300 K). The analysis indicates that the Verwey transition becomes more significant up-core from Subunit Ic to Ib, and stable in Subunit Ia (Fig. 7f). The transition temperature is indistinguishable regardless the magnitude of the demagnetization (Fig. 7c).

## Discussion

### Plagioclase mineralogy of surface sediments in the South Pacific

Our XRD data on chemically separated quartz and feldspars indicate that the upper ~7.4 m of the sediments from Hole U1366C contains albite-rich plagioclase (Fig. 3e). This plagioclase composition is different from the mineralogy reported by Peterson and Goldberg (1962) for coarser fraction (>4 μm), which showed labradolite to andesene composition in the area surrounding Site U1366 from ~170°W to ~130°W. For the entire South Pacific, they report variable plagioclase feldspar composition, but very limited occurrence of albite. We argue that Peterson and Goldberg (1962) may have overlooked fine-grained eolian albite, because they only analyzed grains larger than 4 μm. Similar results were obtained previously for quartz; Peterson and Goldberg (1962) identified large quartz crystals of volcanic origin based on microscopic observation of morphology, while Mokma et al. (1972) showed that bulk quartz exhibits continental oxygen isotope ratios.

### Magnetism and host silicate mineralogy

To a first order, the depth profiles of the relative abundance of silicate minerals (Fig. 4) and magnetism

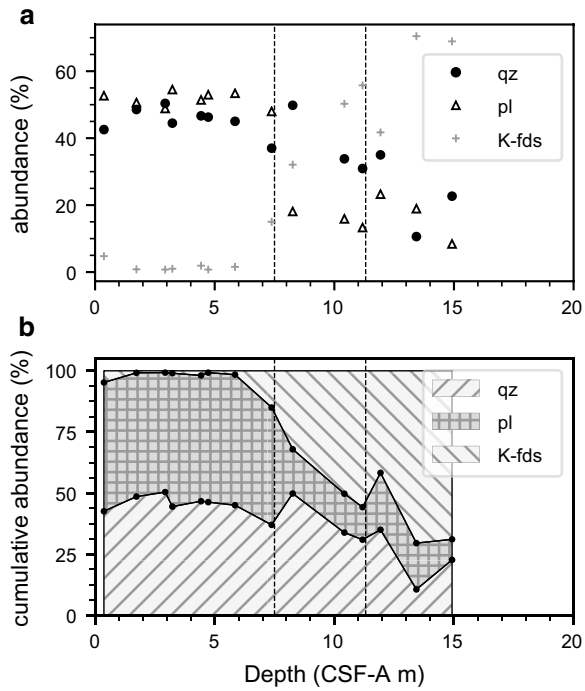


**Fig. 4** Depth variation of silicate mineralogy of the quartz and feldspars separate. **a** Relative abundance of quartz (qz, filled circles), plagioclase (pl, open triangles), and potassium feldspar (K-fds, crosses). **b** Stack plot of the relative abundance. Vertical dashed lines represent lithostratigraphic unit boundaries

(Figs. 5, 6, 7) can be viewed as either monotonic increase or decrease. Therefore, the change in magnetism may reflect mainly the change in the silicate mineralogy, with each silicate has constant magnetic properties throughout the studied interval. While it is also possible that the magnetism of each silicate minerals varies with depth, here we briefly point out the correlations and propose simple models to explain them. Both ARM and SIRM decrease up-core (Fig. 5). This pattern broadly agrees with the decrease of potassium feldspar content and the increase in quartz and plagioclase. Thus, potassium feldspar is likely to be more magnetic per weight than quartz and/or plagioclase. The up-core decrease of the $S_{-0.1}$ values (Fig. 6c) and the increase in demagnetization across the Verwey transition (Fig. 7e) are difficult to explain in a simple way. The $S_{-0.1}$ values imply more impurity and/or finer grain size for upper part, while the Verwey transition suggests the opposite. A possible solution is that quartz and plagioclase accompany different magnetic mineralogy to each other, so that either one of them contains high-coercivity titanomagnetite, while another contains stoichiometric magnetite. This hypothesis, as well as the assumption that the magnetism of each silicate mineral is constant in the studied interval, may be tested by an additional chemical digestion step using $H_2SiF_6$ to separate monomineralic quartz (Syers et al. 1968).

Several studies reported that plagioclase feldspars sometimes contain near-stoichiometric, needle-shaped magnetite exsolutions with high magnetic stability (e.g., Hargraves and Young 1969; Davis 1981; Usui et al. 2006; Wenk et al. 2011; Usui et al. 2015). Such exsolved magnetite exhibits non-interacting single-domain-like behaviors (Evans et al. 1968; Sato et al. 2015) including high

**Table 2 Summary of the magnetic properties of the untreated samples**

| Depth (CSF-A m) | Wet SIRM (A/m) | kARM/SIRM (mm/A) | Dry SIRM ($10^{-2}$ $Am^2/kg$) | $S_{-0.1}$ | $S_{-0.3}$ | Lithostratigraphic unit |
|---|---|---|---|---|---|---|
| 0.37 | 7.314 | 1.11 | 1.43 | 0.90 | 0.97 | Ia |
| 1.43 | 7.8 | 1.17 | Not measured | 0.93 | 0.98 | Ia |
| 1.73 | 7.714 | 1.35 | 1.82 | 0.93 | 0.97 | Ia |
| 2.93 | 6.486 | 1.33 | 1.82 | 0.94 | 0.98 | Ia |
| 3.23 | 8.7 | 1.14 | 2.09 | 0.94 | 0.98 | Ia |
| 4.43 | 8.714 | 1.26 | 1.91 | 0.93 | 0.98 | Ia |
| 4.73 | 9.4 | 1.18 | 2.14 | 0.94 | 0.98 | Ia |
| 5.85 | 12.63 | 0.84 | 3.31 | 0.94 | 0.97 | Ia |
| 7.38 | 7.129 | 2.01 | 1.85 | 0.97 | 0.99 | Ia |
| 8.26 | 9.071 | 1.93 | 2.85 | 0.98 | 0.99 | Ib |
| 8.95 | 7.757 | 1.92 | 3.19 | 0.98 | 0.99 | Ib |
| 10.42 | 14.26 | 2.06 | 3.30 | 0.98 | 0.99 | Ib |
| 11.18 | 12.09 | 2.09 | 3.79 | 0.98 | 0.99 | Ib |
| 11.93 | 13.96 | 2.29 | 3.03 | 0.99 | 1.00 | Ic |
| 13.43 | 23.29 | 2.10 | 4.28 | 0.99 | 1.00 | Ic |
| 14.92 | 12.2 | 1.95 | 4.30 | 0.99 | 1.00 | Ic |

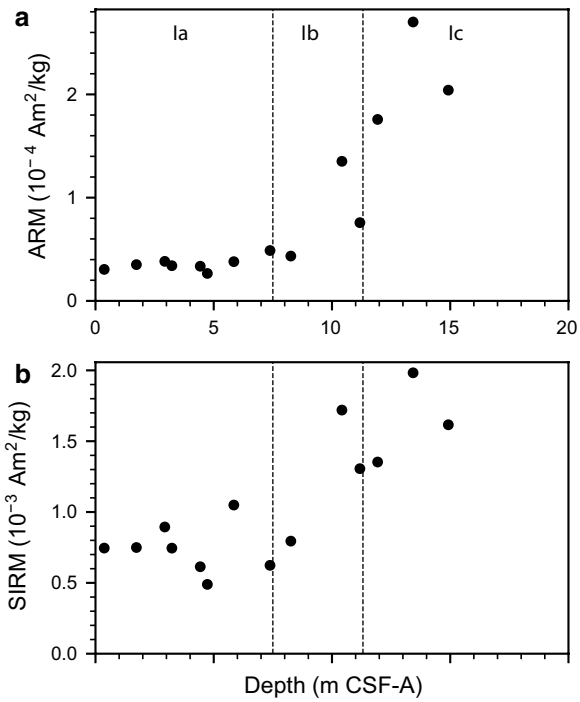


**Fig. 5** Depth variation of remanence intensities of quartz and feldspars; ARM (**a**) and SIRM (**b**). Vertical dashed lines represent lithostratigraphic unit boundaries

kARM/SIRM values of ~2.5 mm/A for a 70 μT DC field for ARM (Cisowski 1981; Usui et al. 2015). The quartz and feldspars studied here show much lower kARM/SIRM. This suggests that exsolved magnetite is not a major remanence carrier in our samples.

It has been assumed that magnetic inclusions in bulk sediments can be characterized by specific magnetic properties such as single-domain signature (Chen et al. 2017) or strong magnetic interactions (Zhang et al. 2018). In this study, even though we exclusively measured magnetism of magnetic inclusions hosted in quartz and feldspars, the magnetic properties vary considerably with depth. This demonstrates that, without direct measurements such as those in this study, or independent evidence for uniformity in magnetic inclusions, it would be difficult to extract the signature of magnetic inclusions from bulk measurements.

### Implication for secular change in eolian component at Site U1366

The changes in the magnetism of the quartz and feldspars observed in this study show both similarities and differences compared to the changes in the contribution of the eolian components estimated by geochemical endmember analysis (Dunlea et al. 2015a). The XRD analyses

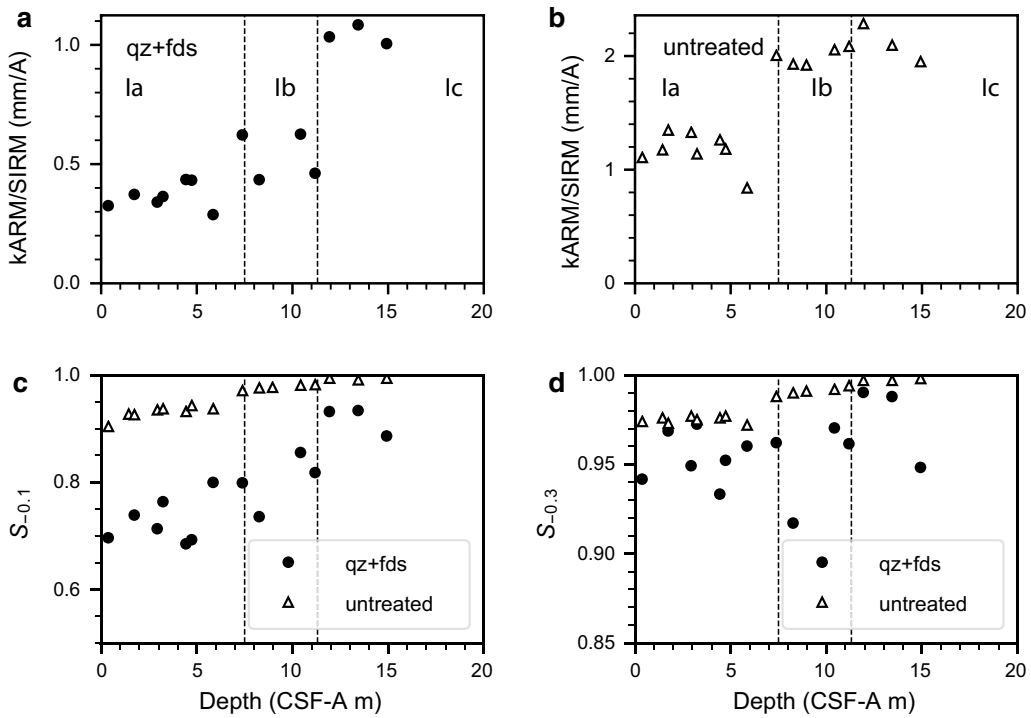


**Fig. 6** Depth variation of magnetic properties. Vertical dashed lines represent lithostratigraphic unit boundaries. **a**, **b** The kARM/SIRM ratios of quartz and feldspars (**a**) and untreated samples (**b**). **c** The $S_{-0.1}$ values of quartz and feldspars (solid circles) and untreated samples (open triangles). **d** The $S_{-0.3}$ values of quartz and feldspars (solid circles) and untreated samples (open triangles)

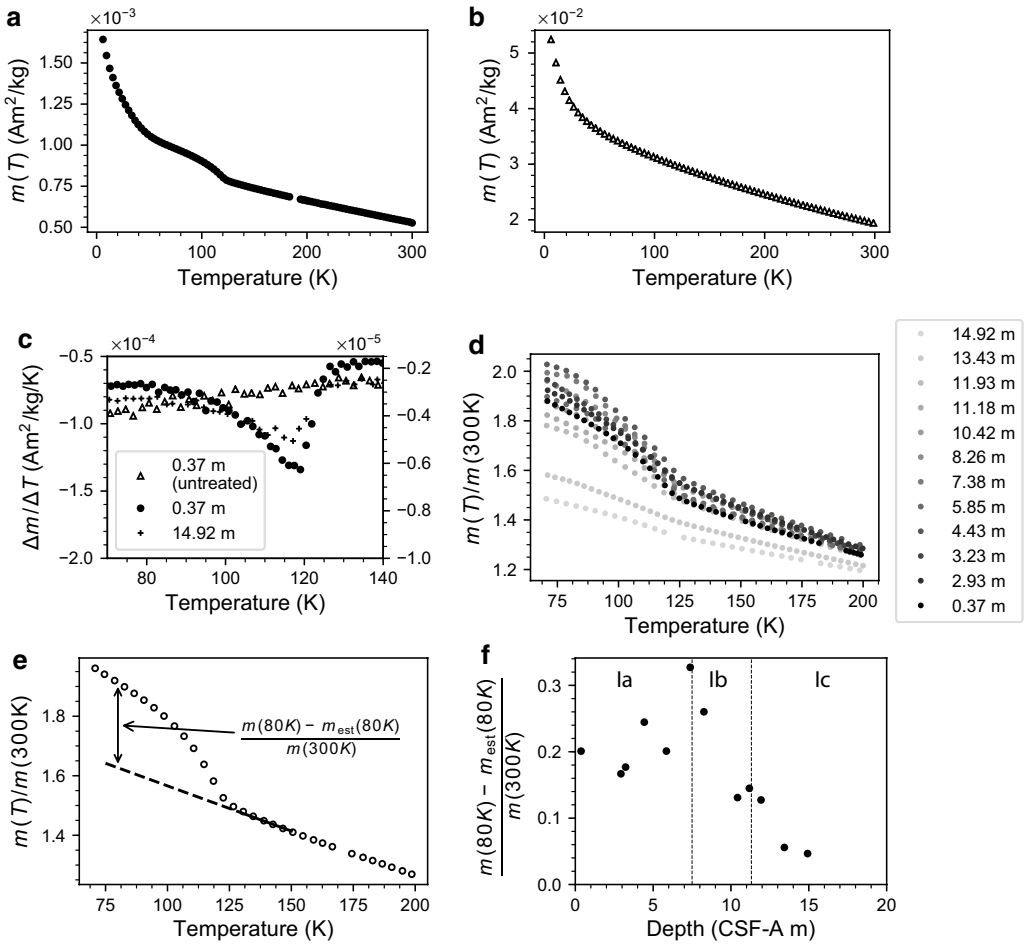


**Fig. 7** Low-temperature magnetism. **a**, **b** Representative thermal demagnetization of low-temperature remanence normalized by the remanence at 300 K of quartz and feldspars (**a**) and untreated sample (**b**) from 0.37 m. **c** Temperature derivative of thermal demagnetization around 120 K highlighting the Verwey transition. Open squares represent untreated samples from 0.37 m (left scale). Solid circles and crosses represent quartz and feldspars from 0.37 and 14.92 m, respectively (right scale). **d** Depth variation of low-temperature demagnetization behavior of the quartz and feldspars around the Verwey transition. **e** The graphical explanation for quantification of the demagnetization across the Verwey transition. **f** The demagnetization across the Verwey transition versus depth. Vertical dashed lines represent lithostratigraphic unit boundaries

indicate that the abundance of albite-rich plagioclase and quartz increases toward the Subunit Ia. These changes correlate with the increase in the "PAAS" end-member to Subunit Ia (Fig. 1), which is likely to come from Australia (Dunlea et al. 2015a). Thus, we interpret that the Australian dust is characterized by either or both of quartz and albite-rich plagioclase. Peterson and Goldberg (1962) argued that plagioclase and potassium feldspar in the South Pacific are volcanic rather than continental origin. If this is the case, the correlation between plagioclase and the "PAAS" end-member may reflect a change in wind pattern to bring both volcanic materials with plagioclase and Australian dust to Site U1366. However, Peterson and Goldberg (1962) only analyzed grains larger than 4 μm that may not be representative of the bulk feldspars, and they did not detect albite-rich plagioclase found in this study. Therefore, it is also possible that albite-rich plagioclase is in the Australian dust. Future investigation of spatial distribution of plagioclase and quartz would help resolving the origin of plagioclase in this region.

The up-core decrease in remanence intensities and disappearance of the potassium feldspar do not match with the geochemical end-member behavior. The contribution of the "PAAS" end-member increases up-core, and the "rhyolite" end-member stays roughly constant in this interval (Fig. 1). These data may be reconciled if there are multiple sources for the "rhyolite" end-member, and if only some of them supply potassium feldspar with abundant magnetic inclusions. The Co-based age model (Dunlea et al. 2015b) suggests that the Subunit Ib/

Ic boundary is 40–70 Ma. If the "rhyolite" end-member represents volcanic ash, it is plausible that volcanic activity changes in tens of millions of years, and that the plate motion brings different volcanic regions closer to the site. In surface sediments of the South Pacific, sanidine has been reported mainly around East Pacific Rise (Murray and Renard 1891; Peterson and Goldberg 1962), so more proximal position to the spreading ridge in the past could explain the presence of potassium feldspar restricted to the deep interval. Additional studies using other proxies such as radiogenic isotopes as well as refinement of chronology will clarify the relationship among mineralogy, magnetism, and geochemistry of the sediments. In any case, these results demonstrate that the magnetic method using magnetic inclusions can provide additional constraints on the provenance of eolian component in pelagic clay.

In Subunit Ib, the mass fraction of quartz and feldspars is low (Fig. 2b). Dunlea et al. (2015a) reported higher contribution of the "Fe–Mn oxyhydroxide" geochemical end-member in Subunit Ib (~ 30–40 wt%). However, the contribution of either "PAAS" or "rhyolite" end-member is not particularly low compared to Subunit Ia or Ic (Fig. 1). Therefore, the low abundance of quartz and feldspars in Subunit Ib cannot be explained by dilution with non-eolian components, and it should reflect characteristics of the eolian component itself. Subseafloor alteration of feldspars may explain the low content of quartz plus feldspars. Dunlea et al. (2015b) estimated slower sedimentation rate of Subunit Ib than Ia, which could promote alteration of feldspars to clay minerals that in turn would dissolve in the chemical digestion. However, the estimated sedimentation rate of Subunit Ib is not slower than Subunit Ic. Thus, we consider subseafloor alteration does not affect significantly the abundance and mineralogy of quartz and feldspars. Alternatively, they may simply reflect the mineralogy of the original eolian dust. It is yet unclear if these characteristics represent the source signature, or they involve sorting during the dust transport. Dubois et al. (2014) reported nearly homogeneous mean grain size of bulk sediments at Site U1366. This might show roughly constant distance to the source and/or wind intensity (Rea 1994). However, the bulk sediments includes authigenic component such as zeolite or biogenic component, so analyses of eolian component (e.g., Rea 1994) or mineral separates (Kawahata et al. 2000) is necessary to constrain the modification during the dust transport.

### Evaluating the importance of magnetic inclusions to sediments magnetism

On the basis of a numerical modeling of remanence acquisition, Chang et al. (2016c) demonstrated that magnetic inclusions can record paleomagnetic signals. Our data represent first direct measurements of remanence intensity of magnetic inclusions in pelagic clay. Although our chemical separation procedure dissolves some candidate host minerals of magnetic inclusions, especially pyroxenes, quartz, and feldspars are often the dominant non-clay minerals in eolian dust (Blank et al. 1985; Leinen et al. 1994) and surface soil (Nickovic et al. 2012). Here, we evaluate the potential contribution of magnetic inclusions to bulk magnetic signals using the remanence intensities of our quartz and feldspars. Our data demonstrate that magnetic inclusions in quartz and feldspars contribute very little (< 1.02% of SIRM) to the bulk magnetism at Site U1366 pelagic clay. This may be due to a high abundance of biogenic magnetite in pelagic red clay (Yamazaki and Shimono 2013; Shimono and Yamazaki 2016; Usui et al. 2017) as suggested by high kARM/IRM of untreated samples. However, the following consideration shows that the contribution of magnetic inclusions to original eolian dust is likely to be small even without the contribution of biogenic magnetite. Shimono and Yamazaki (2016) performed IRM acquisition analysis using log-Gaussian decomposition technique (Kruiver et al. 2001) for sediments from Site U1365 and found that a component relating to biogenic magnetite accounts for 40–65% of SIRM. Assuming that the remaining SIRM is carried by detrital magnetite, and that the magnetic components are similar at Site U1366, this number indicates that magnetic inclusions in quartz and feldspars represent only a few % of remanence carried by detrital magnetite in oxic pelagic sediments. In oxic red clay, the original titanomagnetite would be oxidized to less-magnetic titanomaghemite. Therefore, this number should be viewed as an upper bound. This small number also indicates that direct separation such as chemical digestion applied here is necessary to read the magnetic information carried by magnetic inclusions.

Magnetic inclusions may be more important in reducing environment because reductive diagenesis dissolves discrete detrital magnetic minerals (Chang et al. 2016a). If magnetic inclusions have SIRM intensity of $10^{-3}$ $Am^2/kg$, only 0.1 mg of silicate minerals is required to measure SIRM with standard cryogenic magnetometers. The contribution to natural remanence (NRM) depends on NRM acquisition efficiency; if we assume NRM/SIRM to be 0.1%, 100 mg of silicate minerals would be required to carry measurable NRM.

Recently, Chen et al. (2017) proposed that magnetic inclusions contributed significantly to the total bulk natural remanence in pelagic carbonate from the eastern central equatorial Pacific. They analyzed coercivity distribution of the sediments and showed that detrital magnetic minerals and biogenic magnetite carry similar

SIRM of 0.01–0.02 A/m, respectively, in the sediments. They further argued that the detrital magnetic minerals are inclusions in silicate, based on the single-domain-like behavior and microscopic observation of magnetic separates. Assuming $10^{-3}$ $Am^2/kg$ of SIRM for magnetic inclusions, their estimated SIRM of detrital magnetic minerals is translated to 10–20 mg of silicate per 1 $cm^3$ of bulk sediments. With the average sedimentation rate of 15 mm/kyr determined for the sediments (Chen et al. 2017), this is further translated to inclusion-hosting silicate flux of 15–30 mg/($cm^2$ kyr). This number seems to be too high for equatorial Pacific; the total eolian dust flux including clay minerals to surface sediments is estimated to be around 10–30 mg/($cm^2$ kyr) in this region (Uematsu et al. 1983; Rea 1994; Jacobel et al. 2017), and the quartz and feldspars content in eolian dust is typically ~10–20% (Blank et al. 1985; Leinen et al. 1994). Therefore, we feel that the sediments studied by Chen et al. (2017) also contain discrete magnetic minerals. Nevertheless, the above-mentioned eolian dust flux in the equatorial Pacific and typical quartz and feldspars content suggest that the flux of inclusion-hosting silicate can be ~1–5 mg/($cm^2$ kyr). In this case, our data of SIRM intensity of $10^{-3}$ $Am^2/kg$ indicate that magnetic inclusions may account for tens of % of the SIRM of the sediments studied by Chen et al. (2017). This number is larger than the contribution of the magnetic inclusions to total detrital magnetic minerals estimated earlier for pelagic sediments at Site U1366 (a few %), suggesting that the carbonate studied by Chen et al. (2017) may have experienced reductive diagenesis to reduce the detrital magnetic minerals. Overall, our data support the general conclusion that magnetic inclusions can contribute sediment magnetism significantly (Chang et al. 2016a, c; Chen et al. 2017; Zhang et al. 2018).

## Conclusions

Quartz and feldspars are separated from pelagic red clay from IODP Site U1366 by $Na_2S_2O_7$ fusion technique. These minerals account for 2.3–22.7 wt% of the samples and showed ARM intensity of $3.05 \times 10^{-5}$ to $2.70 \times 10^{-4}$ $Am^2/kg$ and SIRM intensity of $7.45 \times 10^{-4}$ to $1.98 \times 10^{-3}$ $Am^2/kg$. These values account for less than 1.02% of the remanence intensities of untreated samples.

XRD analyses of feldspar mineralogy showed that potassium feldspar is most abundant in Subunit Ic, and albite-rich plagioclase in Subunit Ia. The presence of albite-rich plagioclase differs from a previous regional study (Peterson and Goldberg 1962). We consider this is because the previous study only measures feldspars larger than 4 μm, and overlooked fine-grained eolian albite. The silicate mineralogy and their magnetic properties vary considerably with depth. This warns that bulk measurements alone may be insufficient to separate the signature of magnetic inclusions in sediments.

The up-core increase in the plagioclase and quartz correlates with the increase in the geochemical "PAAS" endember (Dunlea et al. 2015a). We interpret that the quartz and/or albite-rich plagioclase above this interval is transported from Australia via eolian process. This also correlates with the up-core increase in demagnetization across the Verwey transition, suggesting that the quartz and/or plagioclase contains stoichiometric magnetite. The up-core decrease of the potassium feldspar and remanence intensities do not match with the variation of eolian endmembers. We propose that the potassium feldspar traces hidden subdivision of the geochemical "rhyolite" endmember (Dunlea et al. 2015b). Additional study using other provenance fingerprints such as radiogenic isotopes is needed to test this hypothesis.

The remanence intensities of the mineral inclusions studied here indicate that the magnetic inclusions in feldspars and quartz are not important remanence carriers in oxic pelagic sediments; yet, they may be important in anoxic sediments where reductive diagenesis dissolves discrete magnetic minerals. Further investigations using mineral separation techniques on magnetic inclusions are necessary to evaluate the importance of silicate-hosted inclusions to environmental magnetism and paleomagnetism.

#### Abbreviations

JAMSTEC: Japan Agency for Marine-Earth Science and Technology; GSJ: Geological Survey of Japan; PAAS: post-Archean average Australian shale; XRD: X-ray diffraction; SIRM: saturation isothermal remanence; IRM: isothermal remanence; ARM: anhysteretic remanence; NRM: natural remanence; IODP: Integrated Ocean Drilling Program.

#### Authors' contributions

YU designed the study, conducted chemical separation, XRD analysis, and magnetic measurements of feldspars and quartz. TS conducted magnetic measurements of untreated samples. YU, TS, and TY interpreted the data. YU wrote the paper with input from TS and TY. All authors read and approved the final manuscript.

#### Author details

[1] Department of Deep Earth Structure and Dynamics Research, Japan Agency for Marine-Earth Science and Technology, Natsushima-cho, Yokosuka, Kanagawa, Japan. [2] Gas Hydrate Research Laboratory, Meiji University, Kanda-Surugadai, Chiyoda-ku, Tokyo, Japan. [3] Atmosphere and Ocean Research Institute, The University of Tokyo, Kashiwa, Chiba, Japan.

#### Acknowledgements

We thank Dr. Teruhiko Kashiwabara for suggesting measuring magnetism of quartz in sediments. We also thank the editor John Tarduno, the reviewer Dr. Liao Chang, and two anonymous reviewers for constructive comments. This study was performed under the cooperative research program of Center for Advanced Marine Core Research (CMCR), Kochi University (17A063). We thank Prof. Yuhji Yamamoto for help in MPMS measurements at CMCR. This research used samples provided by IODP.

**Competing interests**
The authors declare they have no competing interests.

**Availability of data and materials**
Data are available in Zenodo data repository (https://doi.org/10.5281/zenodo.1414602).

**Consent for publication**
Not applicable.

**Ethics approval and consent to participate**
Not applicable.

**Funding**
This study is supported by JSPS KAKENHI JP17H01361.

## Publisher's Note



Received: 8 May 2018 Accepted: 5 September 2018
Published online: 26 September 2018

**References**

Alekseeva VA, Hounslow MW (2014) Clastic sediment source characterisation using discrete and included magnetic particles—their relationship to conventional petrographic methods in early Pleistocene fluvial–glacial sediments, Upper Don River Basin (Russia). Phys Chem Earth Parts A/B/C 29:961–971

Armbruster T, Bürgi HB, Kunz M, Gnos E, Broenniman S, Lienert C (1990) Variation of displacement parameters in structure refinements of low albite. Am Miner 75(1–2):135–140

Asahara Y, Tanaka T, Kamioka H, Nishimura A, Yamazaki T (1999) Provenance of the north Pacific sediments and process of source material transport as derived from Rb–Sr isotopic systematics. Chem Geol 158(3):271–291. https://doi.org/10.1016/S0009-2541(99)00056-X

Blank M, Leinen M, Prospero JM (1985) Major Asian aeolian inputs indicated by the mineralogy of aerosols and sediments in the western North Pacific. Nature 314(6006):84–86. https://doi.org/10.1038/314084a0

Blatt H, Jones RL, Charles RG (1982) Separation of quartz and feldspars from mudrocks. J Sediment Res 52(2):660–662. https://doi.org/10.2110/jsr.52.660

Bloemendal J, King JW, Hall FR, Doh SJ (1992) Rock magnetism of Late Neogene and Pleistocene deep-sea sediments: Relationship to sediment source, diagenetic processes, and sediment lithology. J Geophys Res Solid Earth 97(B4):4361–4375. https://doi.org/10.1029/91JB03068

Caitcheon GG (1998) The significance of various sediment magnetic mineral fractions for tracing sediment sources in Killimicat Creek. Catena 32(2):131–142

Chang L, Bolton CT, Dekkers MJ, Hayashida A, Heslop D, Krijgsman W, Kodama K, Paterson GA, Roberts AP, Rohling EJ, Yamamoto Y (2016a) Asian monsoon modulation of nonsteady state diagenesis in hemipelagic marine sediments offshore of Japan. Geochem Geophys Geosyst 17(11):4383–4398. https://doi.org/10.1002/2016GC006344

Chang L, Heslop D, Roberts AP, Rey D, Mohamed KJ (2016b) Discrimination of biogenic and detrital magnetite through a double Verwey transition temperature. J Geophys Res Solid Earth 121:3–14. https://doi.org/10.1002/2015JB012485

Chang L, Roberts AP, Heslop D, Hayashida A, Li J, Zhao X, Tian W, Huang Q (2016c) Widespread occurrence of silicate-hosted magnetic mineral inclusions in marine sediments and their contribution to paleomagnetic recording. J Geophys Res Solid Earth 121(12):8415–8431. https://doi.org/10.1002/2016JB013109

Chen L, Heslop D, Roberts AP, Chang L, Zhao X, McGregor HV, Marino G, Rodriguez-Sanz L, Rohling EJ, Pälike H (2017) Remanence acquisition efficiency in biogenic and detrital magnetite and recording of geomagnetic paleointensity. Geochem Geophys Geosyst 18(4):1435–1450. https://doi.org/10.1002/2016GC006753

Cisowski S (1981) Interacting vs. non-interacting single domain behavior in natural and synthetic samples. Phys Earth Planet Inter 26(1–2):56–62. https://doi.org/10.1016/0031-9201(81)90097-2

Clayton RN, Rex RW, Syers JK, Jackson ML (1972) Oxygen isotope abundance in quartz from Pacific pelagic sediments. J Geophys Res 77(21):3907–3915. https://doi.org/10.1029/JC077i021p03907

Cottrell RD, Tarduno JA (1999) Geomagnetic paleointensity derived from single plagioclase crystals. Earth Planet Sci Lett 169(1):1–5. https://doi.org/10.1016/S0012-821X(99)00068-0

Cottrell RD, Tarduno JA (2000) In search of high-fidelity geomagnetic paleointensities: a comparison of single plagioclase crystal and whole rock Thellier–Thellier analyses. J Geophys Res Solid Earth 105(B10):23579–23594

D'Hondt S, Inagaki F, Zarikian CA, Abrams LJ, Dubois N, Engelhardt T, Evans H, Ferdelman T, Gribsholt B, Harris RN, Hoppie BW (2015) Presence of oxygen and aerobic communities from sea floor to basement in deep-sea sediments. Nat Geosci 8(4):299–304. https://doi.org/10.1038/ngeo2387

Davis KE (1981) Magnetite rods in plagioclase as the primary carrier of stable NRM in ocean floor gabbros. Earth Planet Sci Lett 55(1):190–198. https://doi.org/10.1016/0012-821X(81)90098-4

Day R, Fuller M, Schmidt VA (1977) Hysteresis properties of titanomagnetites: grain-size and compositional dependence. Phys Earth Planet Inter 13(4):260–267. https://doi.org/10.1016/0031-9201(77)90108-X

Dubois N, Mitchell NC, Hall IR (2014) Data report: particle size distribution for IODP Expedition 329 sites in the South Pacific Gyre. In: D'Hondt S, Inagaki F, Alvarez Zarikian CA (eds) Proceedings of the IODP, vol 329. Integrated Ocean Drilling Program Management International Inc., Tokyo. https://doi.org/10.2204/iodp.proc.329.201.2014

Dunlea AG, Murray RW, Sauvage J, Spivack AJ, Harris RN, D'Hondt S (2015a) Dust, volcanic ash, and the evolution of the South Pacific Gyre through the Cenozoic. Paleoceanography 30(8):1078–1099. https://doi.org/10.1002/2015PA002829

Dunlea AG, Murray RW, Sauvage J, Pockalny RA, Spivack AJ, Harris RN, D'Hondt S (2015b) Cobalt-based age models of pelagic clay in the South Pacific Gyre. Geochem Geophys Geosyst 16(8):2694–2710. https://doi.org/10.1002/2015GC005892

Dušek M, Petříček V, Wunschel M, Dinnebier RE, Van Smaalen S (2001) Refinement of modulated structures against X-ray powder diffraction data with JANA2000. J Appl Crystallogr 34(3):398–404. https://doi.org/10.1107/S0021889801003302

Evans ME, McElhinny MW, Gifford AC (1968) Single domain magnetite and high coercivities in a gabbroic intrusion. Earth and Planetary Science Letters 4(2):142–146. https://doi.org/10.1016/0012-821X(68)90008-3

Goodyear J, Duffin WJ (1954) The identification and determination of plagioclase feldspars by the X-ray powder method. Mineral Mag 30:306–326. https://doi.org/10.1180/minmag.1954.030.224.03

Grousset FE, Biscaye PE (2005) Tracing dust sources and transport patterns using Sr, Nd and Pb isotopes. Chem Geol 222(3–4):149–167. https://doi.org/10.1016/j.chemgeo.2005.05.006

Hargraves RB, Young WM (1969) Source of stable remanent magnetism in Lambertville diabase. Am J Sci 267(10):1161–1177. https://doi.org/10.2475/ajs.267.10.1161

Hounslow MW, Maher BA (1996) Quantitative extraction and analysis of carriers of magnetization in sediments. Geophys J Int 124(1):57–74. https://doi.org/10.1111/j.1365-246x.1996.tb06352.x

Hounslow MW, Morton AC (2004) Evaluation of sediment provenance using magnetic mineral inclusions in clastic silicates: comparison with heavy mineral analysis. Sediment Geol 171(1–4):13–36. https://doi.org/10.1016/j.sedgeo.2004.05.008

Hubbard CR, Evans EH, Smith DK (1976) The reference intensity ratio, I/Ic, for computer simulated powder patterns. J Appl Crystallogr 9(2):169–174. https://doi.org/10.1107/S0021889876010807

Hunt CP, Singer MJ, Kletetschka G, TenPas J, Verosub KL (1995) Effect of citrate-bicarbonate-dithionite treatment on fine-grained magnetite and maghemite. Earth Planet Sci Lett 130(1–4):87–94. https://doi.org/10.1016/0012-821X(94)00256-X

Hyeong K, Kuroda J, Seo I, Wilson PA (2016) Response of the Pacific intertropical convergence zone to global cooling and initiation of Antarctic glaciation across the Eocene Oligocene Transition. Sci Rep 6:30647. https://doi.org/10.1038/srep30647

Jacobel AW, McManus JF, Anderson RF, Winckler G (2017) Climate-related response of dust flux to the central equatorial Pacific over the past 150 kyr. Earth Planet Sci Lett 457:160–172. https://doi.org/10.1016/j.epsl.2016.09.042

Kawahata H, Okamoto T, Matsumoto E, Ujiie H (2000) Fluctuations of eolian flux and ocean productivity in the mid-latitude North Pacific during the last 200 kyr. Quat Sci Rev 19(13):1279–1291. https://doi.org/10.1016/S0277-3791(99)00096-7

Kruiver PP, Dekkers MJ, Heslop D (2001) Quantification of magnetic coercivity components by the analysis of acquisition curves of isothermal remanent magnetisation. Earth Planet Sci Lett 189(3–4):269–276. https://doi.org/10.1016/S0012-821X(01)00367-3

Kyte FT, Leinen M, Heath GR, Zhou L (1993) Cenozoic sedimentation history of the central North Pacific: Inferences from the elemental geochemistry of core LL44-GPC3. Geochim Cosmochim Acta 57(8):1719–1740. https://doi.org/10.1016/0016-7037(93)90109-A

Lanci L, Delmonte B, Maggi V, Petit JR, Kent DV (2008) Ice magnetization in the EPICA-Dome C ice core: implication for dust sources during glacial and interglacial periods. J Geophys Res Atmos 113(D14):D14207. https://doi.org/10.1029/2007JD009678

Leinen M, Heath GR (1981) Sedimentary indicators of atmospheric activity in the northern hemisphere during the Cenozoic. Palaeogeogr Palaeoclimatol Palaeoecol 36(1–2):1–21. https://doi.org/10.1016/0031-0182(81)90046-8

Leinen M, Prospero JM, Arnold E, Blank M (1994) Mineralogy of aeolian dust reaching the North Pacific Ocean: 1. Sampling and analysis. J Geophys Res Atmos 99(D10):21017–21023. https://doi.org/10.1029/94jd01735

Liu Q, Roberts AP, Larrasoana JC, Banerjee SK, Guyodo Y, Tauxe L, Oldfield F (2012) Environmental magnetism: principles and applications. Rev Geophy 50(4):RG4002. https://doi.org/10.1029/2012rg000393

Liu Q, Sun Y, Qiang X, Tada R, Hu P, Duan Z, Jiang Z, Liu J, Su K (2015) Characterizing magnetic mineral assemblages of surface sediments from major Asian dust sources and implications for the Chinese loess magnetism. Earth Planets Space 67(1):61. https://doi.org/10.1186/s40623-015-0237-8

Lovley DR, Stolz JF, Nord GL, Phillips EJ (1987) Anaerobic production of magnetite by a dissimilatory iron-reducing microorganism. Nature 330(6145):252–254. https://doi.org/10.1038/330252a0

Maher BA (2011) The magnetic properties of Quaternary aeolian dusts and sediments, and their palaeoclimatic significance. Aeol Res 3(2):87–144. https://doi.org/10.1016/j.aeolia.2011.01.005

Maher BA, Watkins SJ, Brunskill G, Alexander J, Fielding CR (2009) Sediment provenance in a tropical fluvial and marine context by magnetic 'fingerprinting' of transportable sand fractions. Sedimentology 56(3):841–861. https://doi.org/10.1111/j.1365-3091.2008.00999.x

Marcille IM, Organova NI, Rozhdestvenskaya IV (1993) Verification of the crystalline structure for sanidines. Vsesoyuznogo Mineralogicheskogo Obshchestva 122(2):85–89

Mokma DL, Syers JK, Jackson ML, Clayton RN, Rex RW (1972) Aeolian additions to soils and sediments in the South Pacific area. Eur J Soil Sci 23(2):147–162. https://doi.org/10.1111/j.1365-2389.1972.tb01650.x

Murray J, Renard AF (1891) Report on deep-sea deposits based on the specimens collected during the voyage of HMS Challenger in the years 1872 to 1876. HM Stationery Office, London

Nakai SI, Halliday AN, Rea DK (1993) Provenance of dust in the Pacific Ocean. Earth Planet Sci Lett 119(1–2):143–157. https://doi.org/10.1016/0012-821X(93)90012-X

Nickovic S, Vukovic A, Vujadinovic M, Djurdjevic V, Pejanovic G (2012) High-resolution mineralogical database of dust-productive soils for atmospheric dust modeling. Atmos Chem Phys 12(2):845–855. https://doi.org/10.5194/acp-12-845-2012

Oldfield F, Maher BA, Donoghue J, Pierce J (1985) Particle-size related, mineral magnetic source sediment linkages in the Rhode River catchment, Maryland, USA. J Geol Soc 142(6):1035–1346. https://doi.org/10.1144/gsjgs.142.6.1035

Petersen N, von Dobeneck T, Vali H (1986) Fossil bacterial magnetite in deep-sea sediments from the South Atlantic Ocean. Nature 320:611–615. https://doi.org/10.1038/320611a0

Peterson MA, Goldberg ED (1962) Feldspar distributions in South Pacific pelagic sediments. J Geophys Res 67(9):3477–3492. https://doi.org/10.1029/JZ067i009p03477

Pettke T, Halliday AN, Hall CM, Rea DK (2000) Dust production and deposition in Asia and the north Pacific Ocean over the past 12 Myr. Earth Planet Sci Lett 178(3):397–413. https://doi.org/10.1016/S0012-821X(00)00083-2

Potter RM, Rossman GR (1979) The manganese-and iron-oxide mineralogy of desert varnish. Chem Geol 25(1–2):79–94. https://doi.org/10.1016/0009-2541(79)90085-8

Rea DK (1994) The paleoclimatic record provided by eolian deposition in the deep sea: the geologic history of wind. Rev Geophys 32(2):159–195. https://doi.org/10.1029/93RG03257

Rea DK, Bloomstine MK (1986) Neogene history of the South Pacific trade winds: evidence for hemispherical asymmetry of atmospheric circulation. Palaeogeogr Palaeoclimatol Palaeoecol 55(1):55–64. https://doi.org/10.1016/0031-0182(86)90137-9

Rea DK, Janecek TR (1981) Mass accumulation rates of the non-authigenic, inorganic, crystalline (eolian) component deep-sea sediments from the western Mid-Pacific Mountains, DSDP Site 463. In: Thiede J, Vallier TL, Adelseck G (eds) Initial reports of the Deep Sea Drilling Project, vol 62. U.S. Government Printing Office, Washington, DC

Rex RW, Goldberg ED (1958) Quartz contents of pelagic sediments of the Pacific Ocean. Tellus. 10:153–159. https://doi.org/10.3402/tellusa.v10i1.9223

Roberts AP (2015) Magnetic mineral diagenesis. Earth Sci Rev 151:1–47. https://doi.org/10.1016/j.earscirev.2015.09.010

Robinson SG (1986) The late Pleistocene palaeoclimatic record of North Atlantic deep-sea sediments revealed by mineral-magnetic measurements. Phys Earth Planet Inter 42(1–2):22–47. https://doi.org/10.1016/S0031-9201(86)80006-1

Sato M, Yamamoto Y, Nishioka T, Kodama K, Mochizuki N, Usui Y, Tsunakawa H (2015) Pressure effect on magnetic hysteresis parameters of single-domain magnetite contained in natural plagioclase crystal. Geophys J Int 202(1):394–401. https://doi.org/10.1093/gji/ggv154

Expedition 329 Scientists (2011) Site U1366. In: D'Hondt S, Inagaki F, Alvarez Zarikian CA, and the Expedition 329 Scientists (ed) Proceeding of the Integrated Ocean Drilling Program, 329. Integrated Ocean Drilling Program Management International, Inc., Tokyo. https://doi.org/10.2204/iodp.proc.329.104.2011

Shimono T, Yamazaki T (2016) Environmental rock-magnetism of Cenozoic red clay in the South Pacific Gyre. Geochem Geophys Geosyst 17(4):1296–1311. https://doi.org/10.1002/2015GC006062

Smith JV (1956) The powder patterns and lattice parameters of plagioclase feldspars. I. The soda-rich plagioclases. Mineral Mag 31(232):47–68. https://doi.org/10.1180/minmag.1956.031.232.05

Stancin AM, Gleason JD, Owen RM, Rea DK, Blum JD (2008) Piston core record of Late Paleogene (31 Ma) to recent seafloor hydrothermal activity in the Southwest Pacific Basin. Paleoceanography 23(1):PA1212. https://doi.org/10.1029/2006pa001406

Stevens RL (1991) Grain-size distribution of quartz and feldspar extracts and implications for flocculation processes. Geo-Mar Lett 11(3–4):162–165. https://doi.org/10.1007/BF02431004

Stolz JF, Chang SB, Kirschvink JL (1986) Magnetotactic bacteria and single-domain magnetite in hemipelagic sediments. Nature 321:849–851. https://doi.org/10.1038/321849a0

Syers JK, Chapman SL, Jackson ML, Rex RW, Clayton RN (1968) Quartz isolation from rocks, sediments and soils for determination of oxygen isotopes composition. Geochim Cosmochim Acta 32(9):1022–1025. https://doi.org/10.1016/0016-7037(68)90067-7

Tarduno JA, Cottrell RD, Smirnov AV (2006) The paleomagnetism of single silicate crystals: Recording geomagnetic field strength during mixed polarity intervals, superchrons, and inner core growth. Rev Geophys 44(1):RG1002. https://doi.org/10.1029/2005rg000189

Thompson R, Oldfield F (1986) Environmental magnetism. Allen and Unwin, London

Uematsu M, Duce RA, Prospero JM, Chen L, Merrill JT, McDonald RL (1983) Transport of mineral aerosol from Asia over the North Pacific Ocean. J Geophys Res C9:5343–5352. https://doi.org/10.1029/JC088iC09p05343

Usui Y, Nakamura N, Yoshida T (2006) Magnetite microexsolutions in silicate and magmatic flow fabric of the Goyozan granitoid (NE Japan): significance of partial remanence anisotropy. J Geophys Res 111(B11):B11101. https://doi.org/10.1029/2005jb004183

Usui Y, Shibuya T, Sawaki Y, Komiya T (2015) Rock magnetism of tiny exsolved magnetite in plagioclase from a Paleoarchean granitoid in the Pilbara

craton. Geochem Geophys Geosyst 16(1):112–125. https://doi.org/10.1002/2014GC005508
Usui Y, Yamazaki T, Saitoh M (2017) Changing abundance of magnetofossil morphologies in pelagic red clay around minamitorishima, Western North Pacific. Geochem Geophys Geosyst 18:4558–4572. https://doi.org/10.1002/2017GC007127
Wenk HR, Chen K, Smith R (2011) Morphology and microstructure of magnetite and ilmenite inclusions in plagioclase from Adirondack anorthositic gneiss. Am Miner 96:1316–1324. https://doi.org/10.2138/am.2011.3760
Yamazaki T, Shimono T (2013) Abundant bacterial magnetite occurrence in oxic red clay. Geol 41(11):1191–1194. https://doi.org/10.1130/G34782.1
Zhang Q, Liu Q, Li J, Sun Y (2018) An integrated study of the eolian dust in pelagic sediments from the North Pacific Ocean based on environmental magnetism, transmission electron microscopy and diffuse reflectance spectroscopy. J Geophys Res Solid Earth. https://doi.org/10.1002/2017JB014951
Zhou LP, Oldfield F, Wintle AG, Robinson SG, Wang JT (1990) Partly pedogenic origin of magnetic variations in Chinese loess. Nature 346:737–739. https://doi.org/10.1038/346737a0